JOURNAL OF MATERIALS SCIENCE 29 (1994) 2641–2647

A functionally gradient coating on carbon fibre for C/Al composites

J. K. YU, H. L. LI, B. L. SHANG
National Laboratory of Solidification Processing, Northwestern Polytechnical University, Xi'an, Shaanxi 710072, People's Republic of China

A functionally gradient coating on carbon fibre for casting C/Al composites with an ultimate tensile strength up to 1250 MPa ($V_f = 0.35$) has been produced. The coating consisted of three layers: an inner pyrocarbon layer, an outer silicon layer and an intermediate gradient layer C/SiC/Si, and their optimum thicknesses were 0.1–0.15, 0.1 and 0.2 μm, respectively. This coating was fabricated by chemical vapour deposition and the C/Al composite was performed by pressure-regulated infiltration. Auger electron spectroscopy and X-ray diffraction analyses confirmed that the structure of the coating was in keeping with its design. The excellent ultimate tensile strength of the C/Al composite also proves that the functionally gradient coating has many functions, including wetting agent, diffusion and reaction barrier, releaser of residual thermal stresses, and tailor of interfacial shear strength. According to the mechanical, physical and chemical coordination between fibre and matrix, the functionally gradient coating can solve nearly all the problems of the interface during fabrication and service.

1. Introduction

The interface is of great importance in carbon fibre-reinforced aluminium matrix composites during fabrication and service. Various methods and ideas have been proposed to control the interface between the fibre and the matrix, thus controlling the performance of C/Al composites. One of the potential methods is fibre coating, which has been given considerable attention since the late 1960s [1–5]. Essentially, three different types of fibre coating have been proposed for C/Al composites. These are metallic coating (nickel, copper) [2, 3], ceramic coating (TiC, SiC) [4, 5] and surface treatment of the fibres by an aqueous solution of a fluoride salt [6]. The various fibre coatings presented above, whether single or double coatings [7, 8], only have limited functions: as wetting agent or diffusion barrier or both [9]. In addition to above two basic requirements, however, fibre coatings should have many other functions, such as releasing residual thermal stresses and adjusting interfacial shear strength, during fabrication and service.

In order to obtain a coating which can suit the complex requirements of the interface, the idea of a functionally gradient coating is presented here. Generally speaking, the design of a functionally gradient coating is based on a given fibre–matrix system. In the present work, interest centred on C/Al composites fabricated by the liquid infiltration method and, in particular, the model of a functionally gradient coating and how the coating is fabricated by chemical vapour deposition (CVD).

2. The model

The fibre coating, as mentioned above, should act as wetting agent, diffusion and reaction barrier, releaser of residual thermal stresses, tailor of interface shear or bonding strength, etc. Obviously, it is impossible to find a single or double coating to meet the challenge. This problem can be solved by a functionally gradient coating which was designed according to the mechanical, physical and chemical coordination between fibre and matrix.

A functionally gradient coating (abbreviated to C/SiC/Si) for C/Al composites is schematically depicted in Fig. 1. The coating consists of three layers. Its inside layer near the carbon fibre is pyrocarbon and its outside layer is pure silicon. The intermediate layer between the pyrocarbon and pure silicon, namely the gradient layer, consists of three sublayers: C/SiC sublayer, SiC sublayer and SiC/Si sublayer. Here, the chemical composition of the C/SiC sublayer changes gradually from 100% pyrocarbon to silicon carbide and the SiC/Si sublayer from silicon carbide to pure silicon. This design makes the functionally gradient coating have many functions.

Wettability in the C/Al system is a major concern for the fabrication of composites by liquid infiltration. Many substances, particularly metallic coatings, have been proposed to act as wetting agents. The most frequently mentioned metal for such coatings is nickel. Nickel reacts strongly with aluminium to form stable intermetallic compounds, however, which is detrimental to the mechanical properties of the C/Al composites [9]. In comparison with the other wetting

0022–2461

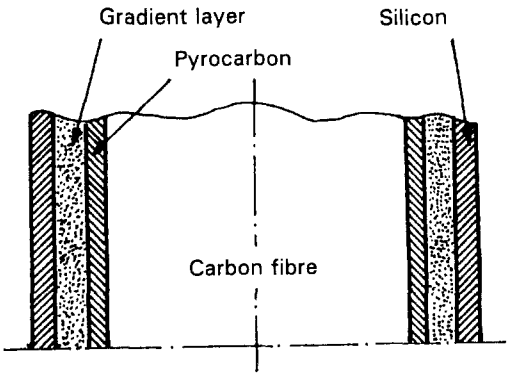

Figure 1 Schematic representation of the model.

agents, silicon has many advantages and is thus selected as the outside layer of the coating. Silicon is one of the quasi-metals and can be wetted easily by aluminium alloys. It is one of the alloying elements in common aluminium alloys and does not react with aluminium to form any detrimental product. In addition, silicon has good oxidation resistance at elevated temperatures, which is important to the coated fibres for preheating during infiltration. Wetting (also bonding) is achieved by mutual dissolution between the silicon layer and the molten matrix. In order to achieve uniform distribution of fibres in the matrix, it is thus necessary to prevent the silicon layer from exhausting before complete solidification of molten matrix. On the other hand, silicon is a brittle material and the remains of the silicon layer should be as thin as possible owing to its detrimental effect on the properties of C/Al composites. The thickness of the silicon layer is directly related, therefore, to the processing variables of liquid infiltration, including fibre preform temperature, T_f, and melt temperature, T_m. For a given range of infiltration parameters (T_f = 823–923 K, T_m = 973–1073 K), the optimum thickness of the silicon layer, d_3, is given by

$$d_3 = 2/3(T_f + T_m) \quad (1)$$

assuming that d_3 is the thickness of the coated silicon layer for the case where the remaining thickness of the silicon layer is from 0.01–0.02 μm. This means that the experimental value of d_3 is approximately 0.1 μm for the C/Al composites fabricated by liquid infiltration.

Another concern for fibre coating is to provide a diffusion and reaction barrier. Silicon coating poorly protects the carbon fibres against attack by molten aluminium due to its rapid dissolution into the matrix. Many ceramic materials have been suggested for the protective coatings, and one of the most efficient coatings was silicon carbide [5, 10]. There is a big mismatch, however, between the coefficient of temperature expansion (CTE) of silicon carbide and that of carbon fibre. This difference of CTE (4.6×10^{-6} and -0.35×10^{-6}, respectively) will cause residual thermal stresses at the interface during fabrication and service, and consequently the concentration of these permanent or transient stresses caused by cracks in the brittle SiC coating will lead to deterioration of the interfacial properties. A possible solution to this problem is to coat intermediate layers on the carbon fibre. If the mismatch of CTE between the adjacent intermediate layers is less than 15%, the residual thermal stress will not deteriorate the interfacial properties [11]. Thus, six or more intermediate layers are necessary. In this case, however, it is difficult to obtain so many intermediate layers in one deposition chamber. The gradient layer, as described above, equals innumerable intermediate layers for matching the difference of CTE, and the great significance is that the former can be fabricated very conveniently and economically. According to Ochiai and Murarami [12], the permissible thickness of a brittle layer, C_I, is calculated from

$$C_I\{F[a/(a + C_I)]\}^2 = G_C^*/\pi\varepsilon_{fu}^2 E_f \quad (2)$$

where a is the radius of the fibre, G_C^* is the strain energy release rate of the fibre, ε_{fu} is the fracture strain of the fibre without brittle layer, E_f is the Young's modulus of the fibre and $F[a/a + C_I)]$ is the geometry correction factor related to relative thickness of the fibre and brittle layer. Silicon carbide is a brittle material and its thickness should be below C_I to prevent the degradation of fibre strength. In the case of PAN II type fibre, the calculated value of C_I is 0.25 μm. Considering the structure of the gradient layer and the remaining thickness (no more than 0.05 μm) of brittle silicon, the selected thicknesses of the three sublayers are 0.05, 0.1 and 0.05 μm, respectively.

The failure mechanisms of fibre-reinforced composites have been extensively investigated over the past two decades [13, 14]. In most reported cases, the reaction products or defects in the matrix will fail at a small strain and circumferential notches will form in this region. If the notches extend into fibres easily, the composite will fracture at low stress. On the other hand, the transverse strength will not be high if the crack tip develops easily along the interface. The interface region should act, therefore, as a tailor of interfacial strength. It has been shown that the crack-tip stresses are very sensitive to the modulus ratio [15]. The tensile stress parallel to the interface increases considerably as the modulus of the cracked phase decreases. Silicon carbide is much stiffer than carbon fibre. This means that the composites reinforced with SiC-coated carbon fibres could fracture at low stress. This problem can be solved by coating a soft pyrocarbon layer between carbon fibre and silicon carbide layer. The soft pyrocarbon layer is beneficial to the longitudinal strength of composites but it is unfavourable to the transverse strength if the layer is too thick. The composite will have high longitudinal strength and better transverse strength if the following sequence exists [16]

$$\sigma_f > \sigma_f^* > \sigma_f^\Delta > \sigma_f^\circ \quad (3)$$

where σ_f is the strength of uncoated fibre, σ_f° is the fibre stress at which a notch is formed on the coated fibre, σ_f^* is the fibre stress at which the notch extends into the fibre, and σ_f^Δ is the debonding strength of the coated fibre. σ_f^Δ can be adjusted by changing the thickness of pyrocarbon layer and the suitable thickness can be obtained by calculation and experiment.

For C/Al composites, the range of thickness is about 0.1–0.15 μm.

3. Experimental procedure

PAN-based carbon fibre was used and each yarn had 1000 filaments. Table I lists the properties of the fibre used. The functionally gradient coating on carbon fibres for C/Al composites was performed by CVD. A cold-wall reactor was used, and the coating could be carried out continuously. Fig. 2 shows a schematic diagram of the CVD apparatus. Liquid $SiCl_4$ (99.99%), C_4H_{10} gas (99.99%), hydrogen gas (99.995%) and argon gas (99.995%) were used as source materials. The liquid $SiCl_4$ was bubbled by argon gas, and then introduced into the reactor. In the cold-wall reactor, carbon fibres were electrically heated under atmospheric pressure, and the temperature field and vapour concentration field were controlled simultaneously. The thickness of the coating was adjusted by temperature field, vapour concentration field and rolling rate. Typical deposition parameters are given in Table II.

The aluminium matrix used was A 356, a common casting alloy with 6%–7.5% Si, 0.3% Mg and 0.3% Fe. Using coated carbon fibres, C/Al composite was fabricated by pressure-regulated infiltration, which is a single-step process. The infiltration chamber was separated into two parts with a spacer into an upper chamber and a lower chamber. An electric crucible for metal melting was located in the bottom of the lower chamber, and the temperature control of the molten metal was maintained with a thermocouple placed in the crucible. A resistance heater located in the upper chamber was placed over a fibre preform mould in which the coated fibres were arranged in bundles. The mould and molten metal were connected with a pipe, and the fibre preform temperature was controlled by a thermocouple placed in the mould at the midpoint of the fibre preform length. The alloy and the fibres were heated to 1050 and 903 K, respectively, and both of the chambers were evacuated to 4000 Pa simultaneously. Compressed air was then directed on to the molten metal and the increasing rates of infiltration pressures (from 0–0.7 MPa) in the chambers were adjusted using the results of dynamic infiltration experiments. The infiltrated metal was solidified under a pressure of 0.7 MPa.

TABLE I Properties of carbon fibre

UTS (MPa)	Young's modulus (GPa)	Failure strain (%)	Density (g cm^{-3})	Diameter (μm)
3300	225	1.55	1.76	6–8

Coated fibres were characterized by scanning electron microscopy (SEM), electron probe microanalysis (EPMA), transmission electron microscopy (TEM), Auger electron spectroscopy (AES) and X-ray diffraction (XRD). Tensile tests of C/Al composites were performed on an Instron 1196 tensile machine at an actuator velocity of 0.5 mm min^{-1}, and for coated carbon fibres, the tests were carried out on a table-model Instron tensile machine at a nominal strain rate of 1 mm min^{-1}. Coated fibres were mounted on cardboard with a gauge length of 80 mm, and the cardboard was cut in the middle after mounting between grips. The specimen geometries of coated fibres and C/Al composites are shown in Fig. 3. The fibre volume fraction, V_f, was determined from specimen weight measurements in air and in a liquid using a laboratory balance and the average thickness of coatings was determined by weight increase of coated fibres.

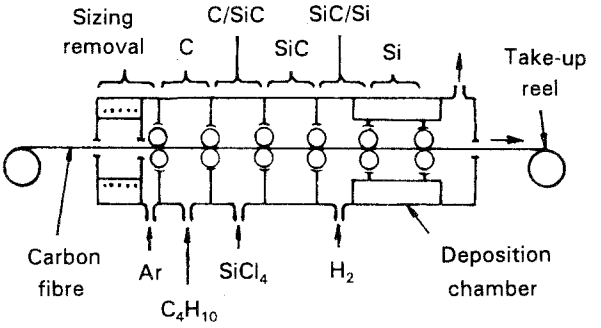

Figure 2 Schematic diagram of the CVD apparatus.

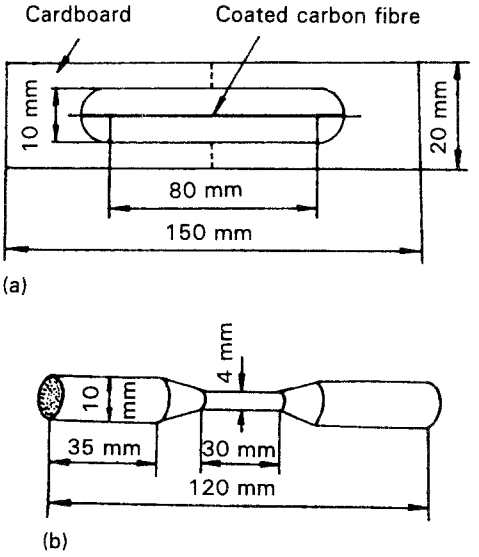

Figure 3 Specimen geometries for tensile tests: (a) coated carbon fibre; (b) C/Al composite.

TABLE II Deposition parameters

Deposition temperature (K)					Gas flow rate (m^3 s^{-1})			
C	C/SiC	SiC	SiC/Si	Si	$SiCl_4$	C_4H_{10}	H_2	Ar
1273	1273–1673	1673	1473–1673	1473	2	0.3	1.4	6

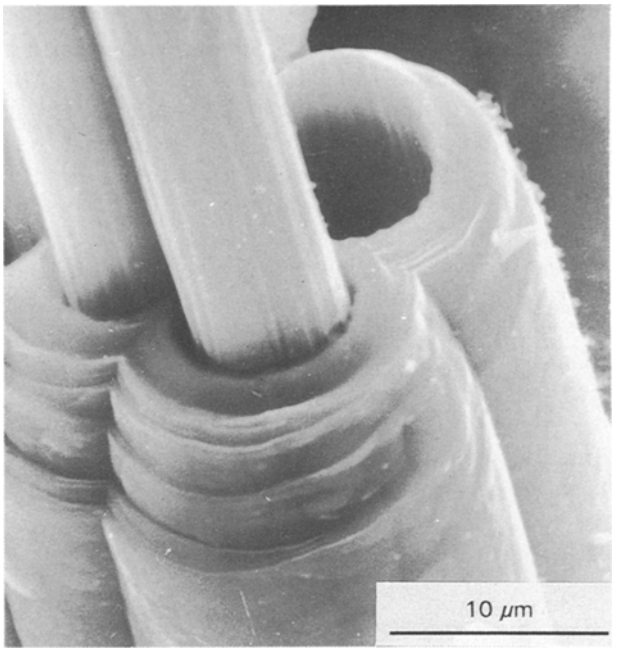

Figure 4 Morphology of the functionally gradient coating on the carbon fibre.

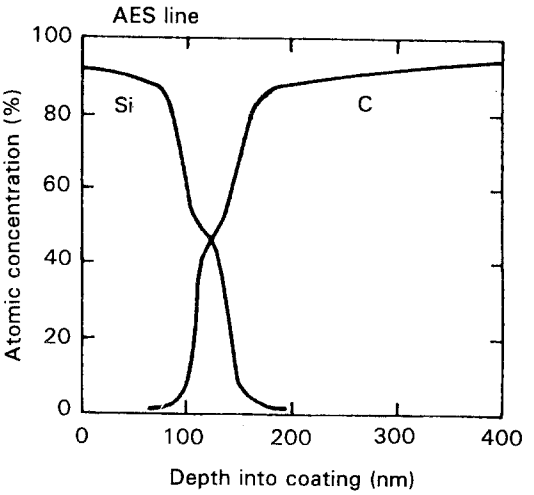

Figure 5 Transverse composition profile of the coated fibre by AES, showing the chemical characterization of the coating.

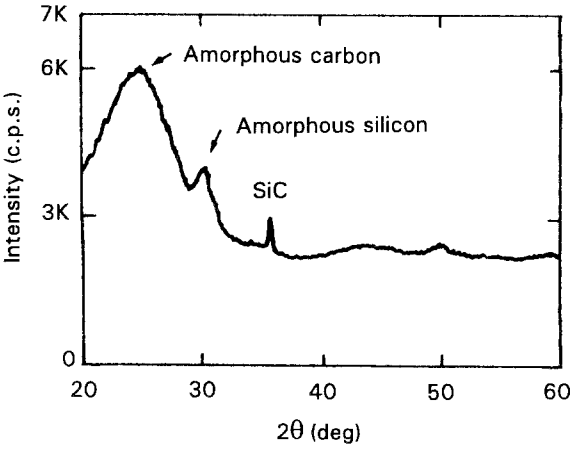

Figure 6 X-ray diffractogram of the functionally gradient coating (CuK_α).

4. Results and discussion

4.1. Microstructure of the coating

The morphology of the functionally gradient coating on carbon fibre is shown in Fig. 4. In order to see the features clearly, the thicknesses of three layers were enlarged during fabrication. This scanning electron micrograph indicates that the coating consists of five layers, and according to the model of the coating, these layers are pyrocarbon, C/SiC sublayer, SiC sublayer, SiC/Si sublayer and silicon, respectively, from inner to outer layer. In fact, there is no evident photographic change from layer to layer if temperature gradients in the deposition chamber change gradually. The stepped change in the coating shown in Fig. 4 is attributed to the sudden change of the temperature gradients between coating sections in the deposition chamber. Fig. 5 shows the transverse composition profile of the coated fibre by AES and it confirms to the chemical characterization of the coating for C/Al composites being in keeping with the design of the coating. Three layers are clearly evident, and the thicknesses of pyrocarbon, the gradient layer and silicon are 0.2, 0.1 and 0.07 μm respectively. The other arrangements of three layers, such as the optimum thicknesses, also show similar chemical characterization. Fig. 6 shows the X-ray diffractogram of the functionally gradient coating. Three layers of the coating consist of amorphous carbon, amorphous or crystalline SiC which is related to the deposition temperatures, and amorphous silicon, respectively. SiC structure is the β fcc, and only the (1 1 1) line is really apparent, showing a preferential orientation of (1 1 1) planes along the pyrocarbon layer. As shown in Fig. 7, each carbon fibre is uniformly and continuously coated. In general, uniformity of the coating includes two types: longitudinal uniformity and transverse uniformity. The former can be easily controlled, while for the latter, it is difficult. The uniformity of the coating expressed in terms of the variation in coating thicknesses can be measured by SEM. For a given thickness of coating, such as 0.5 μm, the variation in thickness along the longitudinal direction of the fibres is no more than 5%. This variation between fibres on the inside of each bundle and those on the outside, however, is up to 20%. In addition, the UTS of coated fibres at room temperature is slightly higher than that of uncoated fibres, showing no degradation of fibres during fabrication.

A functionally gradient coating on carbon fibre was obtained by controlling temperature field and vapour concentration field in the deposition chamber. For the given source vapours, the possible chemical reactions are [17, 18]

$$C_4H_{10}(g) \rightarrow 4C(s) + 5H_2(g)$$

$$\Delta G^\circ = 124\,700 - 365T(\text{J mol}^{-1}) \quad (4)$$

$$4SiCl_4(g) + C_4H_{10}(g) \rightarrow 4SiC(s) + 10HCl(g) + 3Cl_2(g)$$

$$\Delta G^\circ = 1382\,830 - 970.4T(\text{J mol}^{-1}) \quad (5)$$

$$SiCl_4(g) + 2H_2(g) \rightarrow Si(s) + 4HCl(g)$$

$$\Delta G^\circ = 287\,782 - 173.5T(\text{J mol}^{-1}) \quad (6)$$

According to the variation of the Gibbs free energy corresponding to Equations 4–6, pyrocarbon, silicon

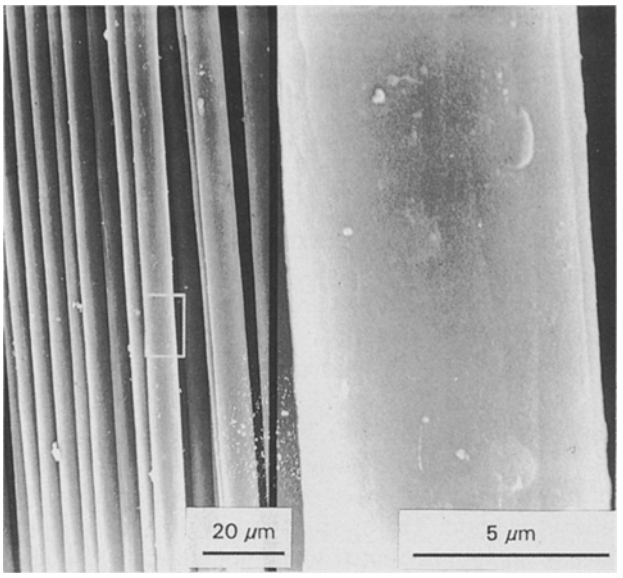

Figure 7 Scanning electron micrograph of the coated fibres, showing the longitudinal uniformity of the coating.

carbide and silicon can be deposited on carbon fibre at 342, 1425 and 1659 K, respectively. In order to obtain quality coatings at high deposition rate, optimum deposition parameters, such as deposition temperature, were investigated. In particular, the temperature field was controlled to make silicon nucleate at high temperature for a very short time, and grow at lower temperatures such as 1273–1473 K. The phenomenon is just the opposite of the solidification of liquid metals, before which liquid metals are supercooled. In contrast to the supercooling of liquid metals, the above phenomenon of silicon nucleation is called "superheating".

Under atmospheric pressure, the composition, morphology and structure of the coating are mainly related to the deposition temperature and vapour concentration. The development of structure in a gradient layer, such as the C/SiC sublayer, which is simultaneously deposited on pyrocarbon layer by carbon and silicon carbide, depends on the temperature field and vapour concentration field between the pyrocarbon layer section and the SiC sublayer section in the deposition chamber. Although no functionally gradient coating on carbon fibres has been proposed before, the structure of other coatings has been investigated extensively. A silicon carbide plus carbon surface layer (called "SCS") of SiC fibres was accomplished by introducing a mixture of hydrocarbon gas and silane vapours, and the microstructure was comprised of an innermost sublayer of amorphous carbon and an outer layer of β-SiC which occurs with the preferred orientation ⟨1 1 1⟩ direction being perpendicular to the substrate [19]. This is consistent with the structure of carbon and silicon carbide in the functionally gradient coating. For the structure of silicon in the coating, co-deposition of free silicon with β-SiC was observed when the deposition temperature was lower than 1673 K [20], although methyltrichlorosilane (CH_3SiCl_3), not $SiCl_4$, was used as a reactant with a fluidizing gas of hydrogen. A striking result was that no deposition of silicon occurred on the carbon fibre at 1473 K although it occurred in the lower temperature zone when a gaseous mixture of $SiCl_4$, hydrogen and argon was used as reactants [8]. Obviously, this is not in agreement with general thermodynamic principles, and our results show that amorphous silicon can be deposited in a wide temperature range from 1273 up to 1773 K. Uniformity of the coating is another important concern for the morphology of the functionally gradient coating. It is proposed that uniformity depends on chemical kinetics in the deposition chamber. Longitudinal uniformity is controlled by temperature, and transverse uniformity by vapour concentration on the fibre surface. Transverse uniformity can be improved, therefore, by lowering the pressure in the deposition chamber.

4.2. C/Al composites

Fig. 8a shows an optical micrograph of a polished cross-section of coated carbon fibres in an aluminium matrix. The coated fibres are completely infiltrated by

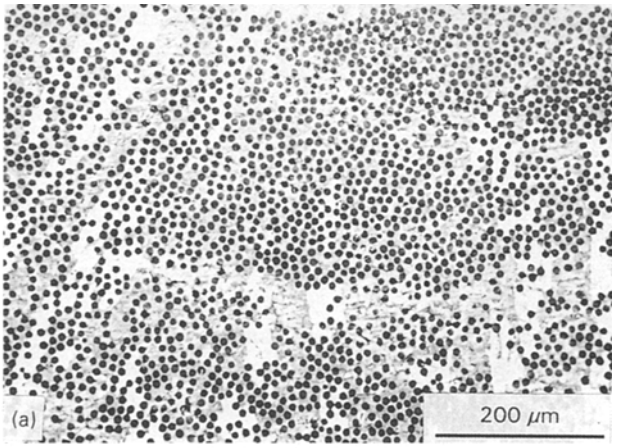

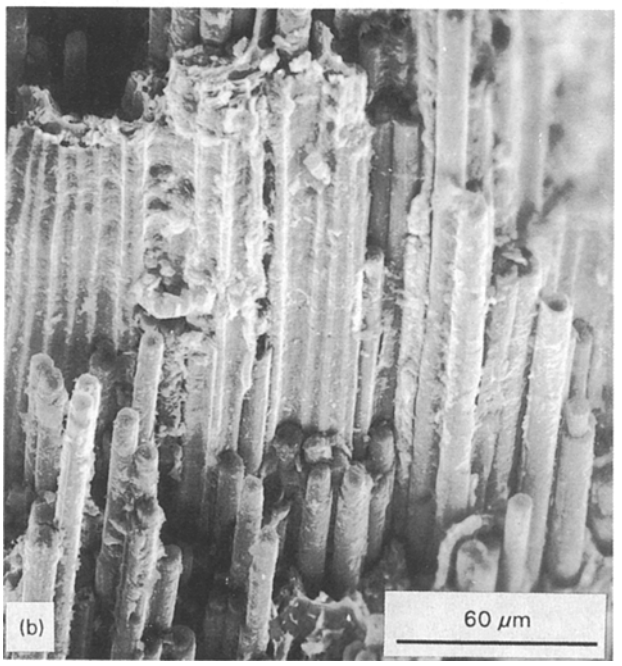

Figure 8 Micrographs of the C/Al composite ($V_f = 0.35$). (a) optical micrograph of a polished cross-section; (b) scanning electron micrograph of the tensile fracture surface.

the aluminium matrix and uniformly distributed over the whole area with nearly no fibre contact. Both XRD and AES detected no detrimental products at the interface between the fibre and the matrix. As shown in Fig. 8b, SEM of the fracture surface of the tensile sample confirmed that fracture had occurred with a modest amount of pull-out of the fibres. EPMA analysis of all the samples revealed that most fibres failed at the pyrocarbon layer between carbon fibre and gradient layer. Fig. 9 shows the effect of the thickness of the coating on the ultimate tensile strength (UTS) of C/Al composites. For each of the three layers, a maximum UTS appears on all the curves, when the thicknesses of two others remain constant. The optimum thicknesses of pyrocarbon layer, gradient layer and silicon layer on the curves (expressed as d_1, d_2 and d_3) are 0.15, 0.2 and 0.1 μm, respectively, and these values are in agreement with the model of the functionally gradient coating. The ultimate tensile strength with different fibre volume fractions and different fibre coatings are presented in Fig. 10 along with the calculated values for the rule of mixtures (ROM). Each data point is the average of at least five tests. The thicknesses of nickel (electroless deposition), silicon carbide in double coating (silicon carbide plus nickel) or functionally gradient coating, silicon and pyrocarbon are 0.2, 0.2, 0.1 and 0.1 μm, respectively. It is noted that the UTS with different fibre coatings increased linearly with increasing V_f. With the exception of the functionally gradient coating, the UTS with fibre coatings could not be described by the ROM. A striking observation from Fig. 10 is that the UTS with single coatings, particularly nickel, was far lower than the ROM value. The results presented above will be discussed next.

For C/Al composites with the functionally gradient coating, wetting is achieved by mutual solution between the silicon layer and the molten aluminium matrix. Good bonding between the fibre and the matrix is obtained, therefore, and no detrimental products at the interface are detected. In the case where carbon fibres are uniformly coated by the functionally gradient coating, the uniform distribution of coated fibres in the matrix is also attributed to a pressure-regulated infiltration process in which the infiltration rate can be controlled. When the thickness of the silicon layer is less than 0.1 μm due to uniformity of the coating, or infiltration processing is slightly changed during fabrication, the silicon layer may be exhausted, causing direct contact between silicon carbide and molten aluminium. Furthermore, silicon carbide can react with molten aluminium at 923 K to produce brittle Al_4C_3 and silicon [21]. No Al_4C_3 is detected at the interface by TEM, however, and a possible reason for this could be that a concentration of dissolved silicon layer at the interface inhibits the above reaction. The morphology of the fracture surface is mainly attributed to the functionally gradient coating, especially the pyrocarbon layer. In fact, the pull-out length can be adjusted by changing the thickness of the pyrocarbon layer in order to obtain the best balance of interfacial properties.

Considering the UTS, there is an optimum thickness of the coating which can be explained by Equations 1–3. When the thickness of the pyrocarbon layer is less than 0.1 μm, $\sigma_f^{\triangle}$ given by Equation 3 becomes higher than σ_f^*, and thus the notch formed cannot change its direction along the interface between pyrocarbon layer and gradient layer but extends into fibres across the pyrocarbon layer. This leads to a lower strength of the composite and a shorter pull-out length of the fibres. When the thickness of the pyrocarbon layer is greater than 0.15 μm, $\sigma_f^{\triangle}$ become lower than the σ_f° given by Equation 3. In this case, the crack is formed in a thick pyrocarbon layer at low stress levels, and leads to a decrease in the UTS of the composite and a very extensive pull-out of the fibres. Similarly, the optimum thicknesses of the gradient layer and the silicon layer can be interpreted by

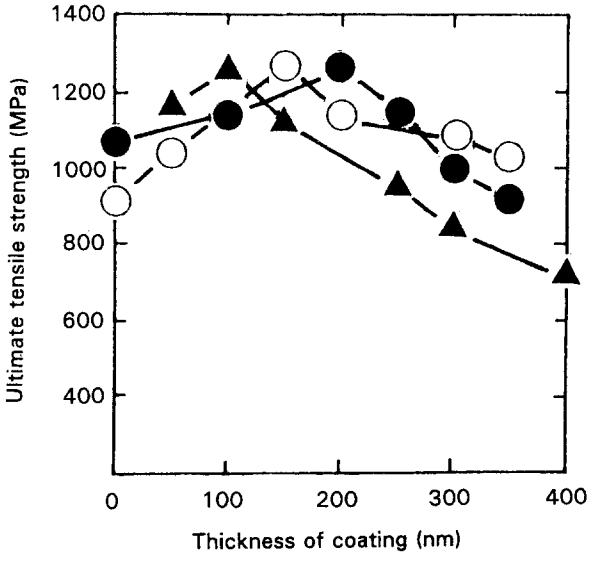

Figure 9 Effect of the thickness of the coating on the ultimate tensile strength for C/Al composite. (○) Pyrocarbon layer (d_2 = 0.2 μm, d_3 = 0.1 μm); (●) gradient layer (d_1 = 0.15 μm, d_3 = 0.1 μm); (▲) silicon layer (d_1 = 0.15 μm, d_2 = 0.2 μm).

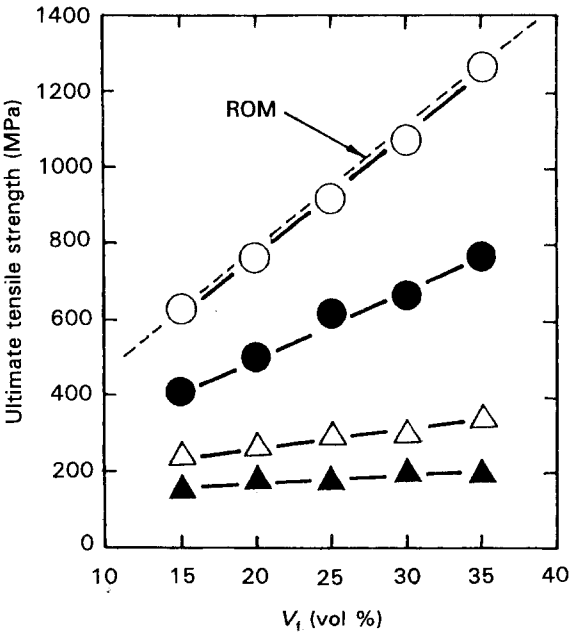

Figure 10 Ultimate tensile strength as a function of fibre volume fraction for C/Al composite, together with calculated values for the rule of mixtures. (▲) Ni, (△) Si, (●) SiC + Ni, (○) C/SiC/Si.

Equations 2 and 1 in Section 2, respectively. From Fig. 10, it can be concluded that the coating types play an important role in C/Al composites. Double coatings are better than single coatings because silicon carbide acts as a diffusion barrier, and a nickel coating is worse than a silicon coating due to the formation of brittle products such as Ni_3Al, NiAl, $NiAl_3$, etc. [9, 22]. The high UTS of C/Al composites with the functionally gradient coating is attributed to the many functions of the coating, including wetting agent, diffusion and reaction barrier, releaser of residual thermal stresses, and tailor of interfacial shear strength. It should be noted that the idea of the functionally gradient coating can be applied to other composite systems, such as C/Mg composites [23].

5. Conclusions

1. The functionally gradient coating for C/Al composites has many functions, including wetting agent, diffusion and reaction barrier, releaser of residual thermal stresses, tailor of interfacial shear strength, etc. This coating can solve nearly all the problems of the interface during fabrication and service. Similar coatings could also be applied to other composite systems.

2. Using chemical vapour deposition, the coating can be fabricated conveniently. The structure and properties of coated fibres also prove that CVD is a successful method for this coating.

3. The optimum thicknesses of the pyrocarbon layer, the gradient layer and the silicon layer are 0.1–0.15, 0.2 and 0.1 μm, respectively, and using coated fibres, the C/Al composite with a UTS up to 1250 MPa ($V_f = 0.35$) has been successfully fabricated by pressure-regulated infiltration.

Acknowledgement

This research was sponsored by the National Natural Science Foundation of China under contract 58971069.

References

1. T. W. CHOU, A. KELLY and A. OKURA, *Composites* **16** (1985) 187.
2. F. A. BADIA and P. K. ROHATGI, *AFS Trans.* **77** (1969) 402.
3. B. C. PAI, A. G. KULKARNI and N. BALASUBRAMANIAN, *J. Mater. Sci.* **14** (1979) 592.
4. K. PHILLIPS, A. J. PERRY, H. E. HINIERMANN and H. GASS, *ibid.* **6** (1971) 271.
5. L. AGGOUR, E. FITZER, M. HEYM and E. IGNATOWITZ, *Thin Solid Films* **40** (1977) 97.
6. J. P. ROCHER, J. M. QUENISSET and R. NASLAIN, *J. Mater. Sci.* **24** (1989) 2697.
7. M. F. AMATEAU, *J. Compos. Mater.* **10** (1976) 279.
8. K. HONJO and A. SHINDO, *J. Mater. Sci.* **21** (1986) 2043.
9. F. DELANNAY, L. FROYEN and A. DERUYTTERE, *ibid.* **22** (1987) 1.
10. A. G. METCALFE, in "Composite Materials, Vol. 1, Interfaces in metal matrix composites", edited by L. J. Broutman and R. H. Krock (Academic Press, New York, London, 1974) p. 1.
11. J. J. GEBHARDT, in "Proceedings of the 3rd International Conference on CVD", edited by F. A. Glaski (Electrochemical Society, Princeton, NJ, 1972) p. 369.
12. S. OCHIAI and Y. MURARAMI, *Metall. Trans.* **12A** (1981) 684.
13. T. U. MARSTON and A. G. ATKINS, *J. Mater. Sci.* **9** (1974) 447.
14. J. E. KING, *Met. Mater.* **5** (1978) 720.
15. A. G. EVANS, M. RULE and B. J. DALGLEISH, *Metall. Trans.* **21A** (1990) 2419.
16. S. OCHIAI and K. OSAMURA, *ibid.* **18A** (1987) 673.
17. K. K. YEE, *Int. Met. Rev.* **23**(1) (1978) 19.
18. L. Z. CHENG, "Physical Chemistry" (Shanghai Science and Technology Press, Shanghai, 1988) in Chinese.
19. F. W. WAWNER, A. Y. TENG and S. R. NUTT, *SAMPE Q.* April (1983) 39.
20. K. MINATO and K. FUKUDA, *J. Mater. Sci.* **23** (1988) 699.
21. V. LAURENT, D. CHATAIN and N. EUSTATHOPOULOS, *ibid.* **22** (1987) 244.
22. J. K. YU, H. L. LI, B. L. SHANG and H. W. WANG, *J. Xi'an Inst. Metall. Construct. Eng.* **24** (1992) 105 (in Chinese).
23. K. ZHANG, J. K. YU and Z. Y. MAO, in "Proceedings of the 9th International Conference on Composite Materials", Vol. 1, edited by A. Miravete (Woodhead Publishing Ltd., Cambridge, UK, 1993) p. 565.

Received 4 May
and accepted 29 October 1993